Wake Flow Simulations for a Mid-Sized Rim Driven Wind Turbine

Andrew B. Porteous[1], Bryan E. Kaiser[2], and Svetlana V. Poroseva[3]
University of New Mexico, Albuquerque, New Mexico, 87131

Cody R. Bond[4]
University of Texas at Austin, Austin, Texas, 78712

Rob O. Hovsapian[5]
Idaho National Laboratory, Idaho Falls, Idaho, 83415

The onshore land where wind farms with conventional wind turbines can be placed is limited by various factors including a requirement for relatively high wind speed for turbines' efficient operation. Where such a requirement cannot be met, mid- and small-sized turbines can be a solution. In the current paper, simulations of near and far wakes behind a mid-sized Rim Driven Wind Turbine (U.S. Patent 7399162) developed by Keuka Energy LLC is analyzed. The purpose of this study is to better understand the wake structure for more efficient wind farm planning. Simulations are conducted with the commercial CFD software StarCCM+.

Nomenclature

D = *turbine diameter*
R = *blade length*
Re_D = *Reynolds number based on the turbine's diameter*
U = *mean velocity in the streamwise flow direction*
U_∞ = *free stream wind velocity in the streamwise direction*
k = *turbulent kinetic energy*
ρ = *air density*
τ_w = *wall shear stress*
u_τ = *friction velocity* $\sqrt{\tau_w/\rho}$
y^+ = *dimensionless distance from the wall based on fluid properties* yu_τ/ν
ν = *kinematic viscosity*

I. Introduction

CONVENTIONAL Horizontal Axis Wind Turbines (HAWT) are most efficient at relatively high free stream wind velocity. HAWT's typically have a large hub height, in the 100 m range[10], to increase the swept area and reduce ground and freestream wind interactions. The average freestream wind speed required for large scale HAWT efficient

[1]Graduate student, Mechanical Engineering, MSC01 1105, 1 UNM Albuquerque, NM 87131-0001, AIAA Student Member.
[2]Graduate student, Mechanical Engineering, MSC01 1105, 1 UNM Albuquerque, NM 87131-0001, AIAA Student Member.
[3]Assistant professor, Mechanical Engineering, MSC01 1105, 1 UNM Albuquerque, NM 87131-0001, AIAA Associate Fellow.
[4]Undergraduate student, Mechanical Engineering, MSC01 1105, 1 UNM Albuquerque, NM 87131-0001, AIAA Student Member. Status at the time of conducting research.
[5]Scientist, Idaho National Laboratory, Idaho Falls, ID 83415-3810.

operation[1] is around 15 ms^{-1}. This high wind speed requirement greatly impacts inland areas suitable for construction of wind farms.

If to consider, for example, the state of New Mexico, the average wind speed here is in Category 3. Figure 1 shows seasonal variations of the wind speed at 40 m above the ground. The data shown in the figure is a subset of the larger database of vector-averaged horizontal wind speeds and directions at various heights from 30 m to 120 m collected over a two year span at 10-minute intervals, from August 1, 2010 to July 31, 2012 at GPS coordinates 34.981283N 106.551733W (near Albuquerque). The database was generated by post-processing observational data released to our research group for academic use by Organization 4143, Environmental Programs, of Sandia National Laboratory. The raw data was collected by a Model VT-1 Phased-Array Doppler Sonic Detection and Ranging (SODAR) system, owned and operated by Sandia National Laboratories. The data post-processing was performed using Microsoft Access and MATLAB commercial software. The two years of data were averaged together to represent a single year; then, the 10-minute periods were averaged into hour blocks. A smoothing spline algorithm was applied to generate 3D surfaces at different heights. For data shown in Fig. 1, the total average wind speed is 4.15 ms^{-1}. Similar estimates were made for all available heights that allowed us to confirm low average wind speeds at this location.

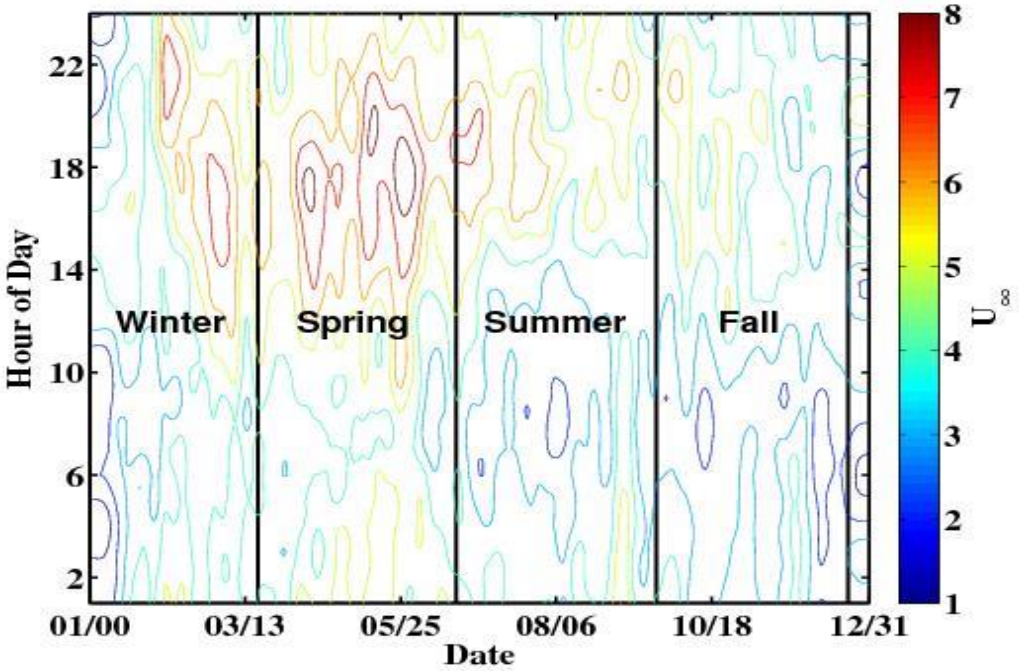

Figure 1: Seasonal wind speed variation in Albuquerque NM at 40m (year 2011)

In areas with low wind speeds, small- to mid-sized wind turbines can be beneficial. In our study, the performance of the Keuka Rim-Driven Wind Turbine (RDWT) (U.S. Patent 7399162) developed by Keuka Energy LLC is analyzed using tools of the computational fluid dynamic (CFD) analysis. This is a mid-sized turbine, which is currently in production and testing stage. The objective is to predict the complex flow structure formed around and behind the turbine in a range of low average wind speeds characteristic for states like Florida, New Mexico, and Texas.

The Keuka RDWT is a drag-driven wind turbine designed for wind energy extraction in locations of average wind class three or below. The design is passive-stall-controlled for simplicity and lower capital expense. It features high solidity (16 blades) and is power-rated[2] at 15kW. The turbine diameter considered in this study is approximately 7.62 m. A rope is threaded around the entire rim of the turbine and through two direct drive variable high speed generators[1]. This unique rope drive contains pulleys with five grooves that the rope is wrapped around. The hub height of the turbine can be adjusted for reduced maintenance cost and to capture the maximum possible wind energy. The turbine is schematically shown in Fig. 2.

The complex structure of a flow around RDWT presents many challenges for conducting reliable and accurate numerical solutions. Turbine operation over a broad range of Reynolds numbers, interaction with atmospheric turbulence, and the presence of dynamic stall are just a few challenges to overcome. Appropriate computational grid resolution requirements render Direct Numerical Simulations (DNS) and Large Eddy Simulations (LES) computationally unfeasible for such simulations. The Reynolds-Averaged Navier-Stokes (RANS) turbulence model

provides an alternative approach to the computationally expensive DNS and LES models. RANS models are typically used to model far wakes of wind turbines[3] and are readily available in many computational fluid dynamic CFD software packages. In this study, the shear stress transport (SST) turbulence model[4] and the k-ω 2006 model[5] are used to simulate wake flow behind RDWT. The near-wake flow structure analysis and quantitative predictions of the turbine's thrust and power were made in our previous studies[6,7]. A sensitivity analysis to simulation parameters will be conducted. Another objective of the current study is to analyze the effect of initial conditions on results of simulations. Typically, an initial wind speed profile is assumed to be uniform.

Computations were conducted using commercial CFD software, STAR CCM+ by CD-adapco[8].

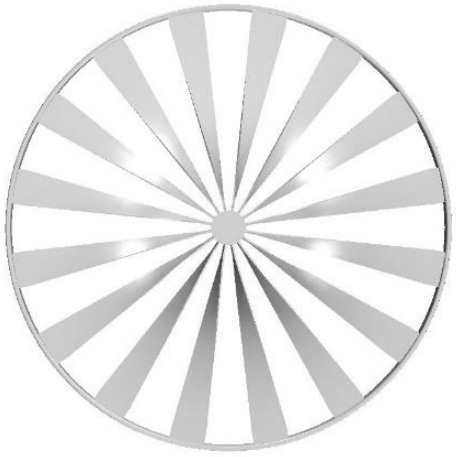

Figure 2: The Keuka Wind Turbine, front view.

II. Simulation Parameters

A. Computational Domain

An initial domain size of 10Dx10Dx10D in length, width, and height directions, respectively, is chosen as the control volume to simulate a flow around and behind RDWT. Currently, the turbine is located at the mid-height of the computational domain. Simulations with larger computational domains are conducted to evaluate the sensitivity of simulation results to the boundaries placement. First, the height (+y direction) is increased by 5D while the width and wake dimensions are held constant. Then, the total width (±z direction) is increased to 15D while the height and wake dimensions are held constant. Finally, the wake (+x direction) is increased by 5D while the height and width dimensions are held constant. The four domains are represented in Fig. 3.

The computational domain and grids were generated in Star-CCM+[8].

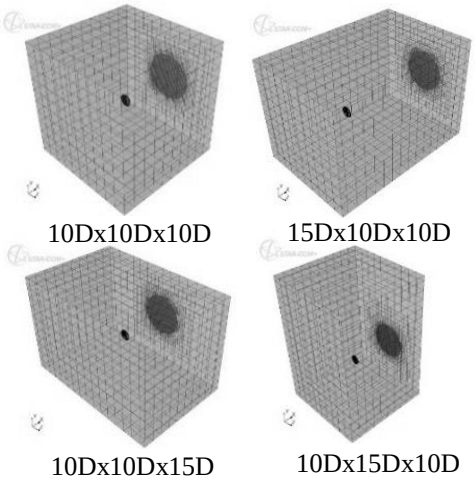

Figure 3: Domain sizes.

B. Grids

In the current study, two different types of grids are used to analyze the effect that an *unstructured* mesh and a *structured* grid have on simulation results in near and far wakes. The unstructured mesh is composed of cells and structured grids are composed of hexahedral cells. The minimum size of cells closest to the wind turbine surface was chosen to be in the range from 5 to 50 mm. The size of cells adjacent to the computational domain boundaries was set to be two diameters (2D). The cell density varies through the domain in all meshes, with the smallest cells being at the wind turbine to capture the high-gradient zones.

The polyhedral mesh has a growth rate of 1.6, and the cell density is of 0.75. This mesh includes 0.8 million cells and its schematic is shown in Fig. 4. More detail on the mesh generation can be found in Ref. 7. The hexahedral grid

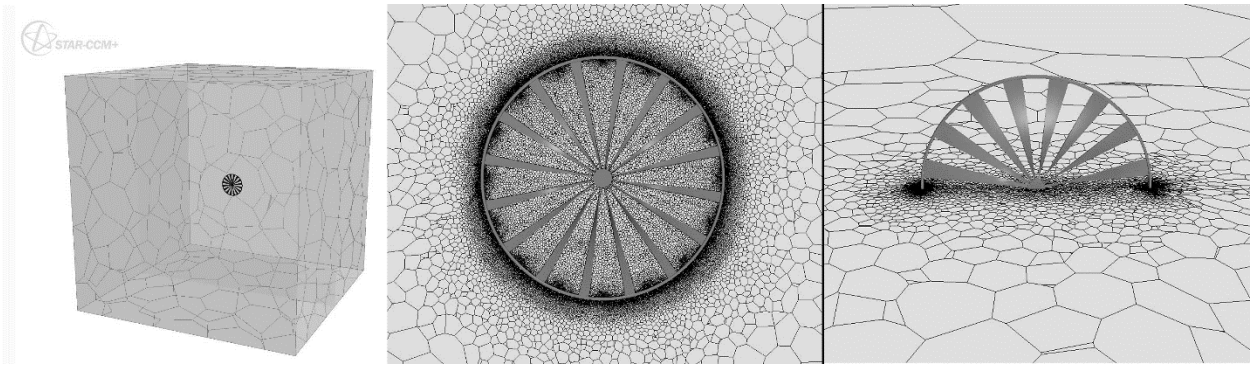

Figure 4: Computational polyhedral mesh.

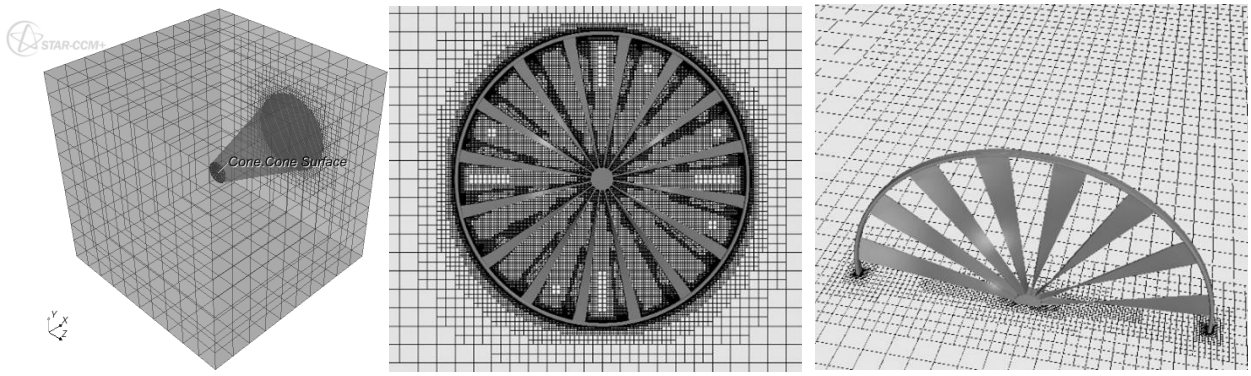

Figure 5: Structured grid and wake refinement.

is shown in Fig. 5. In this grid, anisotropic distribution of square cells was implemented with the base size of one diameter (1D) and the stretching ratio of 1.1. To resolve the complex structure of the wake flow, the volumetric control is implemented as the sub-domain in the main grid. The sub-domain's grid is made of isotropic square cells at 10% of the base size. The sub-domain geometry is a conic section with the smallest diameter of 1D at $1/32$ D placed in front of the turbine and the largest diameter of 2D placed at the end of the main domain (Fig. 5). A set of structured grids was used in the current study for sensitivity analysis. The largest grid, 15Dx10Dx10D, includes 1.4 million cells. Other grids contain 1.2 million cells.

III. Boundary Conditions

A uniform inlet velocity (+x direction) equal to the free stream wind speed is assigned as the inlet condition. The freestream wind velocity is assigned 6 ms^{-1} corresponding to the Reynolds number (based on turbine diameter) of 3 million. The angular velocity of the wind turbine is set to 5.1468 rad/s in correspondence with the values obtained from the RDWT prototype at the aforementioned free stream wind speeds[2]. The no-slip condition is placed on the turbine with the adiabatic thermal condition and smooth wall surface specifications.

A pressure outlet condition is applied to the boundary in the wake with a prescribed gage pressure of zero. All other planes that limit the computational domain are treated as symmetry planes. The turbine tower was not represented in simulations.

IV. Numerical Method

Computations were conducted using commercial software STAR CCM[8]. First- and second-order upwind calculation for the convection term is available in Star-CCM+[8]. The stability and accuracy of the numerical scheme is greatly affected by the selected method. The method used in this work is the second-order upwind numerical scheme.

V. Turbulence Models

RANS turbulence models for the current study were determined by the sensitivity analysis results conducted in our previous research[6,8,9]. The SST and k-ω 2006 turbulence models[4,5] were found to produce the most reliable results

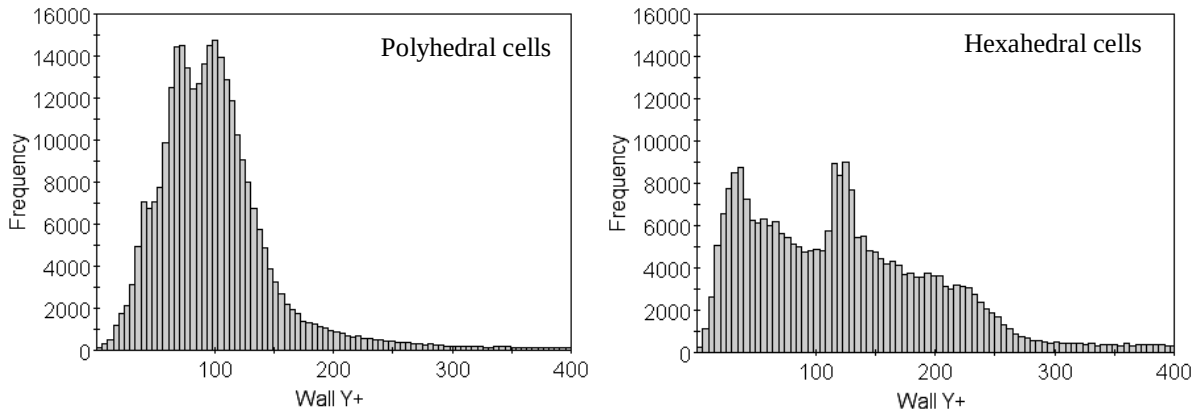

Figure 6: Wall y^+ histograms at a free stream wind velocity of 6 ms^{-1}.

for this case. Both models are used with the two-layer all y^+ wall treatment option which uses the initial cell y^+ value, from the wall of the wind turbine, to determine if the y^+ value is in the log layer. If the y^+ valve is greater than 30, it is assumed that the wall y^+ value is in the log layer and wall functions are used to satisfy the flow conditions. If the y^+ values are 1 or less the viscous sublayer is assumed to be resolved and no wall functions are used.

VI. Results

Histograms of the frequency of the wall cell y^+-values are shown in Fig. 6 for the *unstructured* (polyhedral) mesh and the *structured* (hexahedral) grid. Relatively large computational domains and the complex geometry cause large variations in the wall cell y^+ value. This justifies the implementation of the all y^+ wall treatment available in Star-CCM+ for the selected turbulence models.

A study was conducted to determine the effect that *unstructured* and *structured* grids have on the simulation results. Vertical profiles of the mean velocity in the streamwise direction are shown in Figs. 7 and 8. There is the separation region close to the turbine hub (Fig.7). The dynamics of mean streamwise velocity profiles with the distance downstream the turbine are given in Fig. 8. In the near wake ($x/D < 1$), velocity profiles obtained with structured and unstructured grids are in acceptable agreement with each other. A difference between the simulation results obtained using different grids increases with the distance from the turbine.

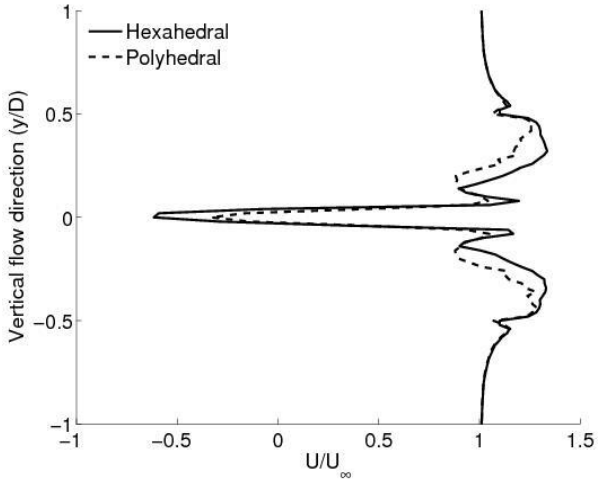

Figure 7: Mean wake velocity profile behind the turbine at 0.05D.

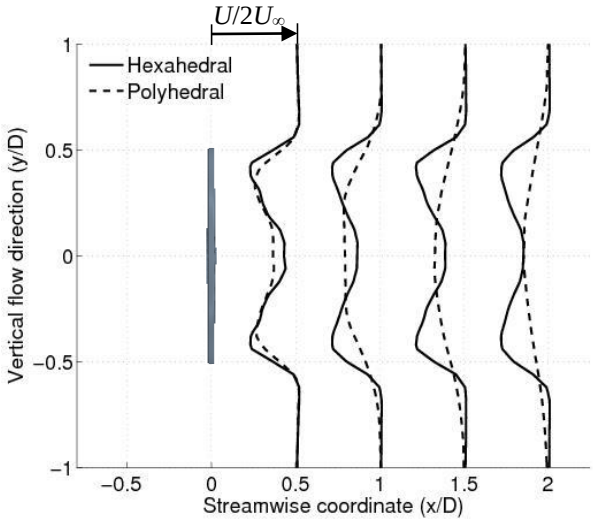

Figure 8: Mean wake velocity profiles at different locations behind the turbine.

The hexahedral grid captures the flow geometry much better than the polyhedral grid does at $x/D > 1$. In simulations with the unstructured mesh, the far wake vanishes fast, which is in contradiction with observations. Figures 9-12 show the velocity and the turbulent kinetic energy contours obtained with the unstructured mesh and the structured grid. These figures give an opportunity to visually compare the simulated wakes behind the turbine. Unphysical results for the far wake are clearly seen when the unstructured mesh is used. Simulation results shown in Figs. 7-12 were obtained with the Menter's SST turbulence model[4].

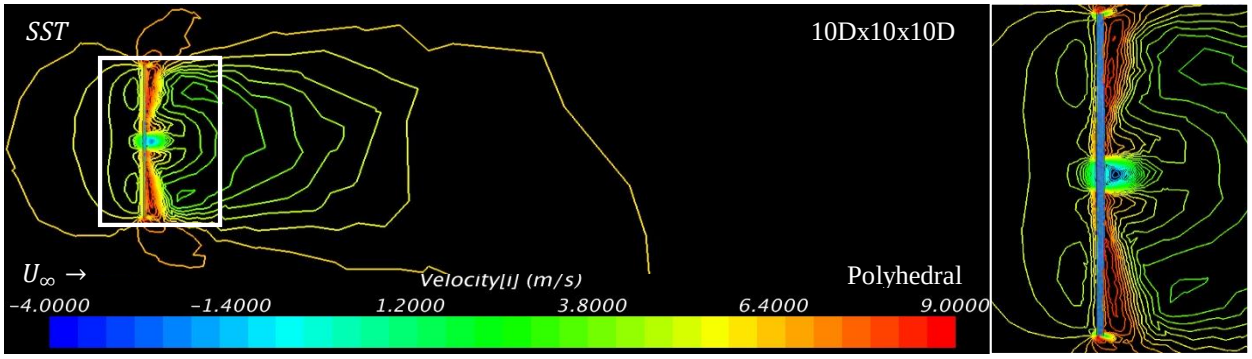

Figure 9: Mean streamwise velocity contours: *unstructured* mesh.

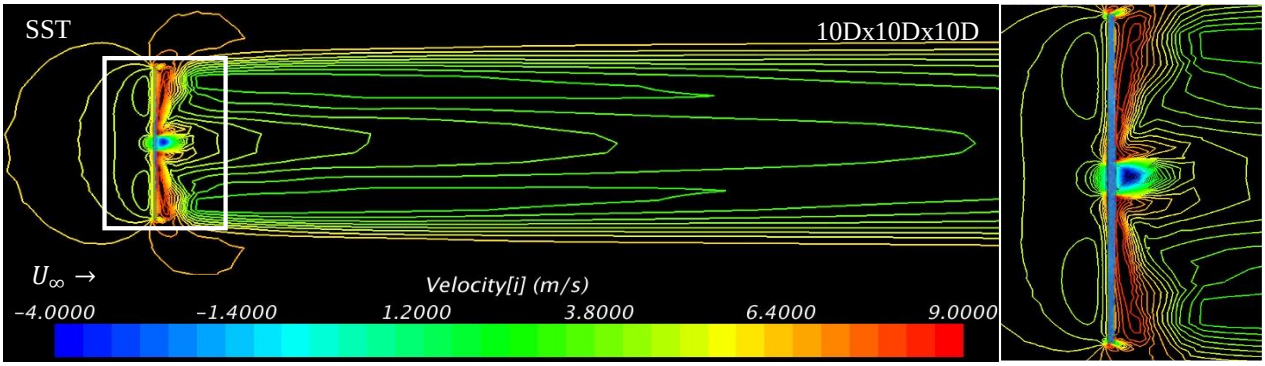

Figure 10: Mean streamwise velocity contours: *structured* grid.

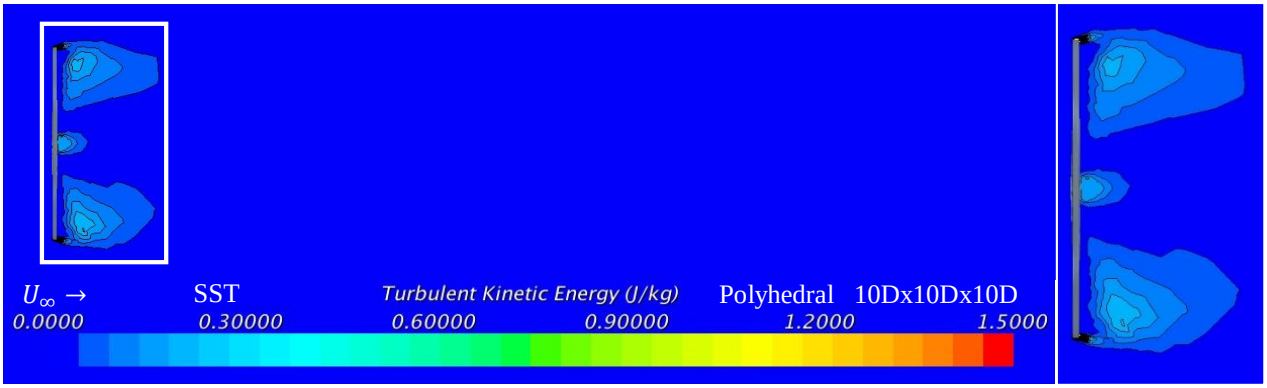

Figure 11: Turbulent kinetic energy contours: *unstructured* mesh.

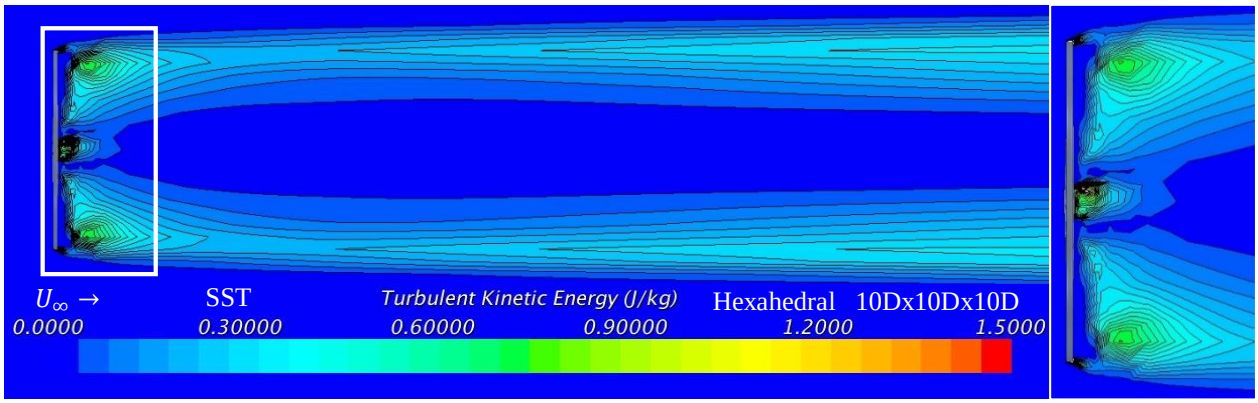

Figure 12: Turbulent kinetic energy: *structured* grid.

Because the simulations conducted with the structured grid produce more realistic results, the structured grids were used in the following simulations.

At the next step, the analysis was conducted to determine how the computational domain size affects the simulation results. The Menter's SST turbulence model[4] was used in simulations. Figure 13 shows the effect that the domain size has on the near-wake vertical profiles of the mean streamwise velocity and the turbulent kinetic energy. The velocity profiles at 1D behind the turbine are in close agreement for different domains. The turbulent kinetic energy profiles although similar, differ in magnitude for different domains. The profiles obtained in the 15Dx10Dx10D domain deviate the most from others. This result is expected as in the longest domain in the streamwise direction, the influence of the outlet boundary conditions on the simulation results should be the least.

The mean velocity and turbulent kinetic energy profiles at 5D behind the turbine are shown in Fig. 14. Observations are similar to those made for Fig. 13. That is, the simulation results obtained in the longest domain in the streamwise direction deviate mostly from the profiles obtained in other domains. The wake progression of the mean streamwise velocity component and that of the turbulent kinetic energy are given in Fig. 15.

The mean streamwise velocity contours obtained in computational domains of different sizes are given in Figs. 16-19. These figures confirm the similarity of the near-wake flow structures obtained in different domains and demonstrate a noticeable difference in the far wake structure when the longest 15Dx10Dx10D domain is used.

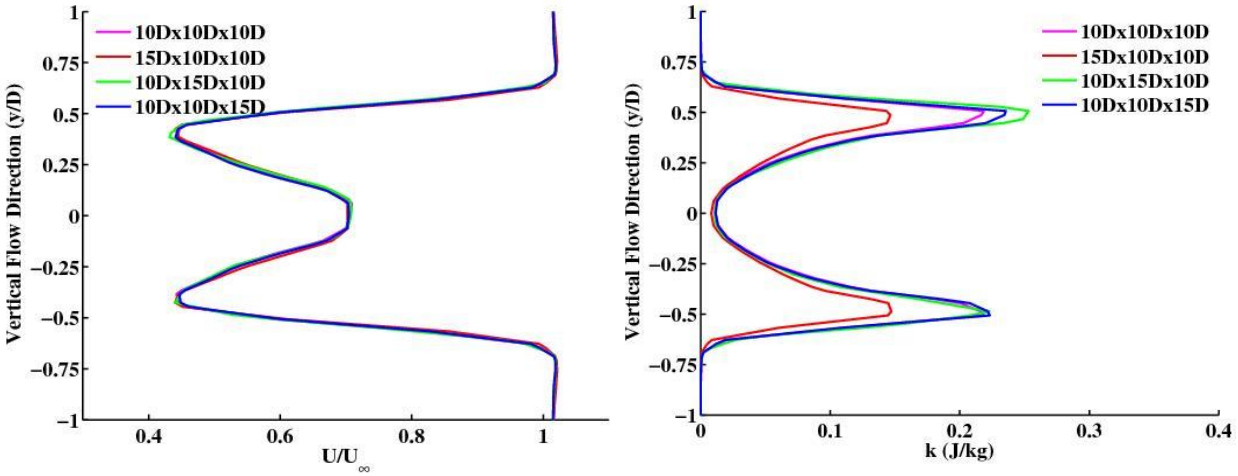

Figure 13: Vertical profiles of U and k at 1D behind turbine.

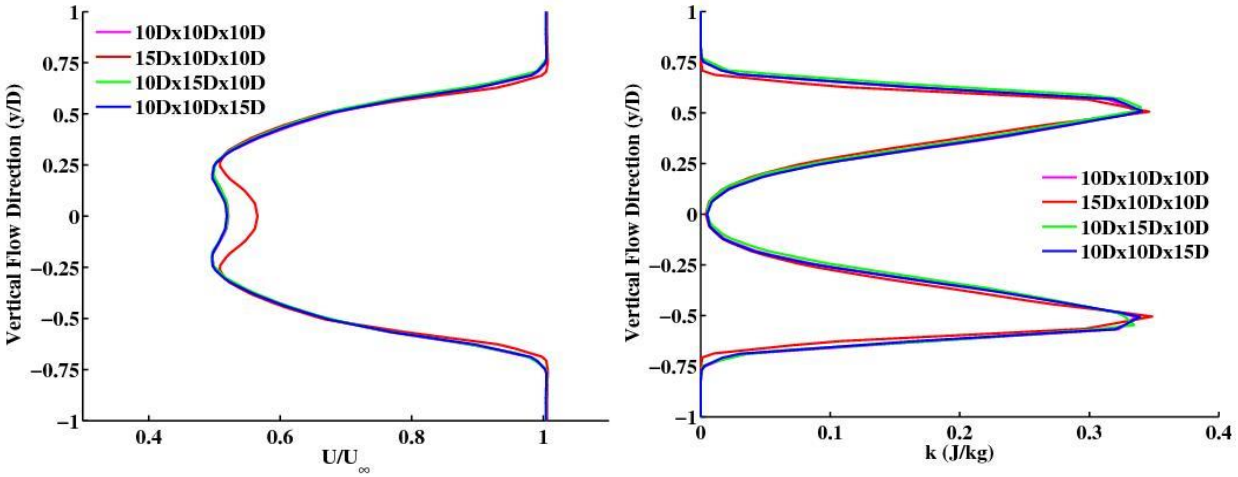

Figure 14: Vertical profiles of U and k at 5D behind turbine.

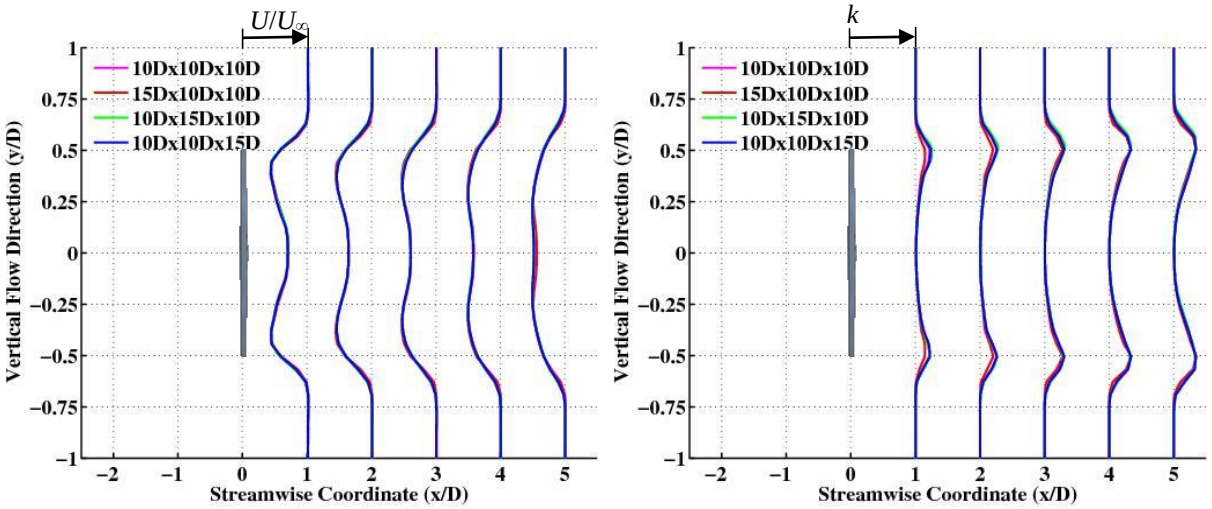

Figure 15: Vertical wake profile for $U_\infty = 6ms^{-1}$

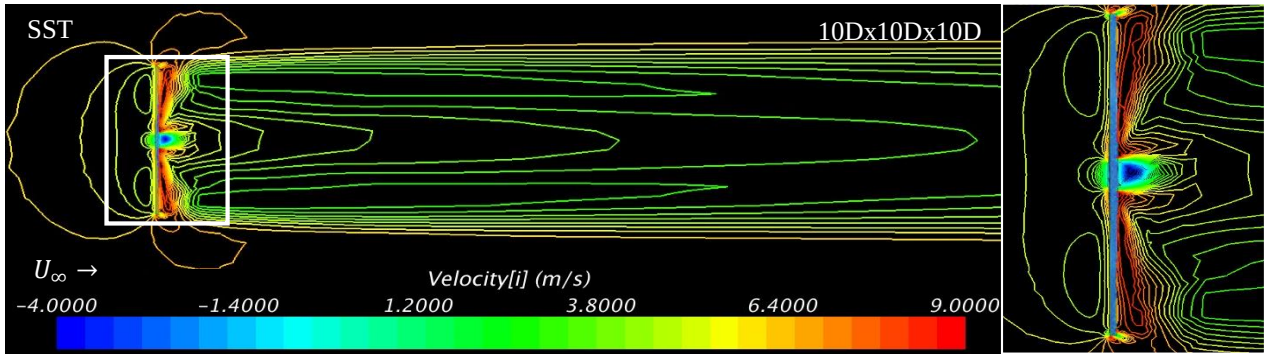

Figure 16: Mean streamwise velocity contours: 10Dx10Dx10D domain.

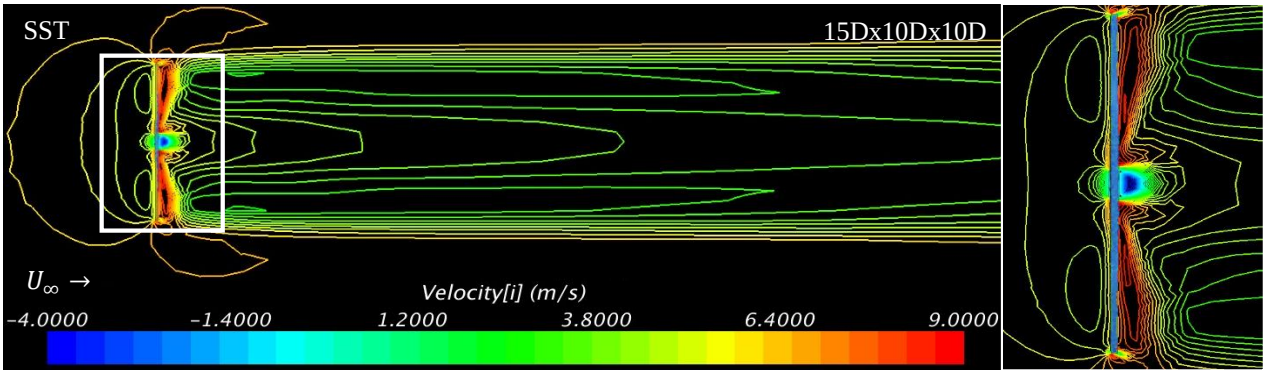

Figure 17: Mean streamwise velocity contours: 15Dx10Dx10D domain.

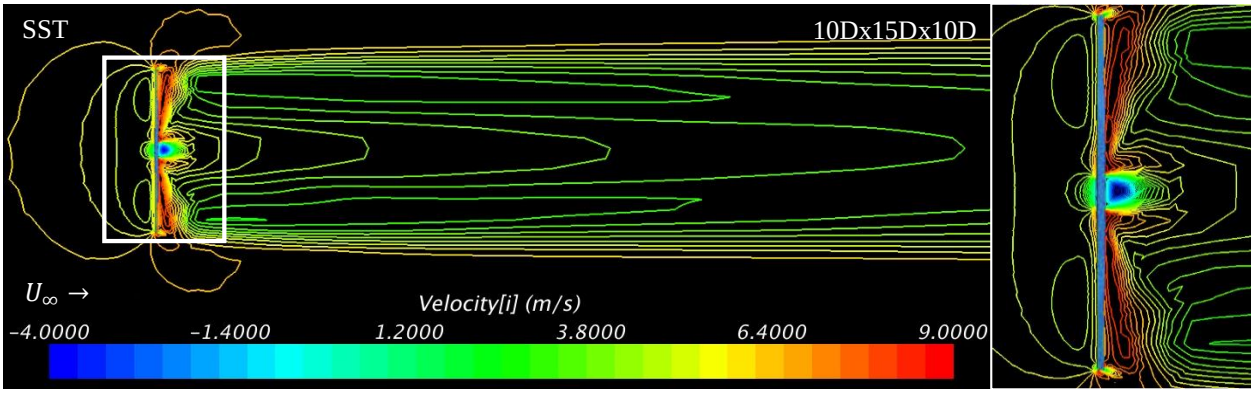

Figure 18: Mean streamwise velocity contours: 10Dx15Dx10D domain.

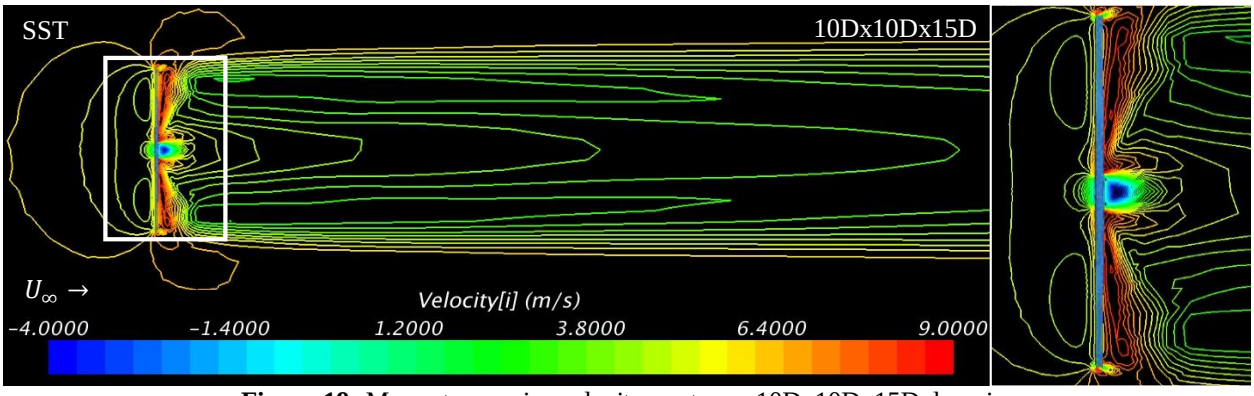

Figure 19: Mean streamwise velocity contours: 10Dx10Dx15D domain.

The results presented in Figs. 13-18 are expectedly sensitive to the length of the computational domain in the steamwise direction. They are over-predicted for the mean velocity and the turbulent kinetic energy in shorter domains to compare with the profiles in the longer domain. However, in the absence of accurate observational data to compare the simulation results with, the smallest (and the least computationally expensive) domain, 10Dx10Dx10D, can be used for the analysis of the flow structure in the near wake of the turbine. The reliable far-wake simulations require a larger domain in the streamwise direction.

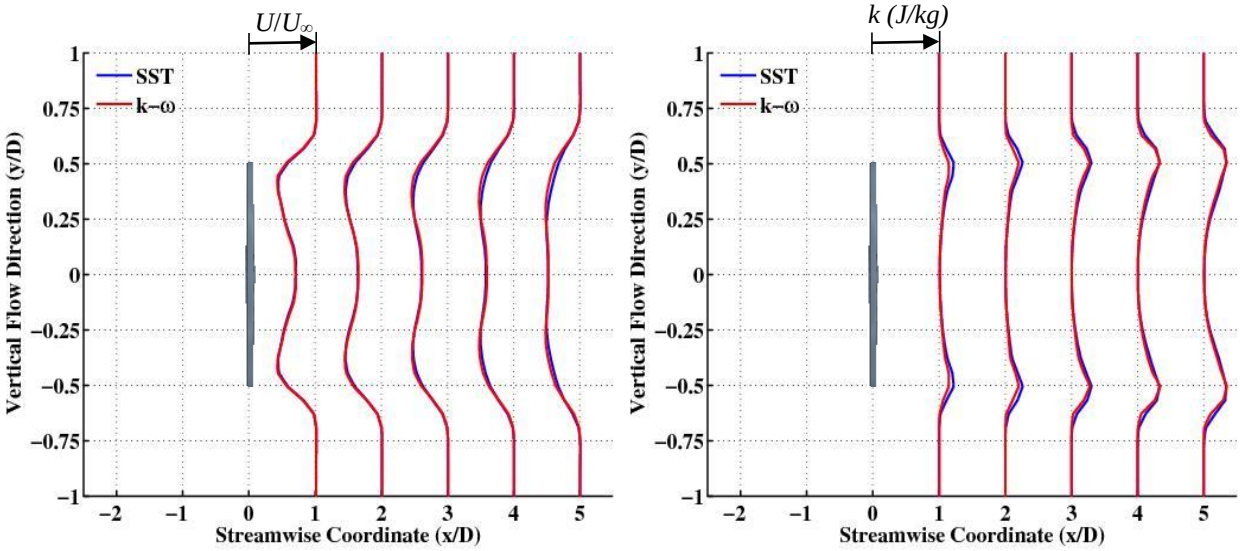

Figure 20: Velocity and turbulent kinetic energy profiles.

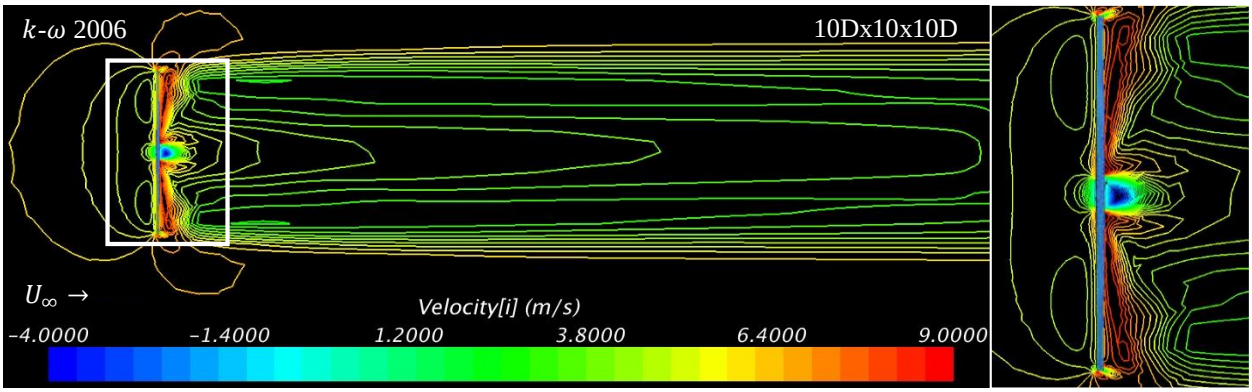

Figure 21: Contour of mean streamwise velocity using the *structured* grid for $U_\infty = 6ms^{-1}$ (k-ω 2006)

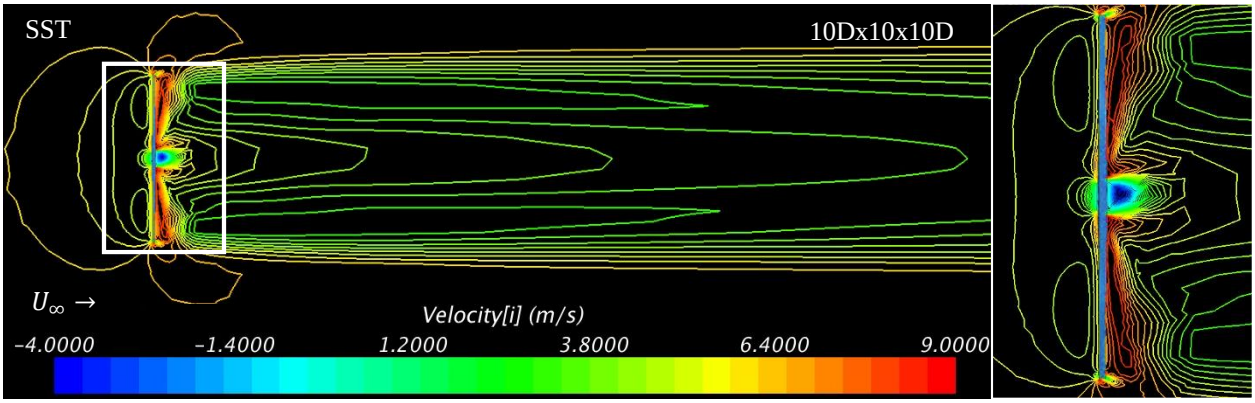

Figure 22: Contour of mean streamwise velocity for $U_\infty = 6ms^{-1}$ 10Dx10Dx10D (SST)

The simulation results obtained with the different turbulence models are compared in Fig. 20. Simulations were conducted with the SST and k-ω 2006 turbulence models[4,5] In the figure, the wake progression is shown. Simulations were conducted in the 10Dx10Dx10D domain. The streamwise velocity profiles are in close agreement with each other in the near wake and differ in magnitude in the far wake. The difference in results is more noticeable in Figures 21 and 22, where the mean streamwise velocity contours obtained with the SST and k-ω 2006 turbulence models are shown.

In Figure 23, vorticity contours obtained with the Menter's SST turbulence model in the 10Dx10Dx10D domain are presented.

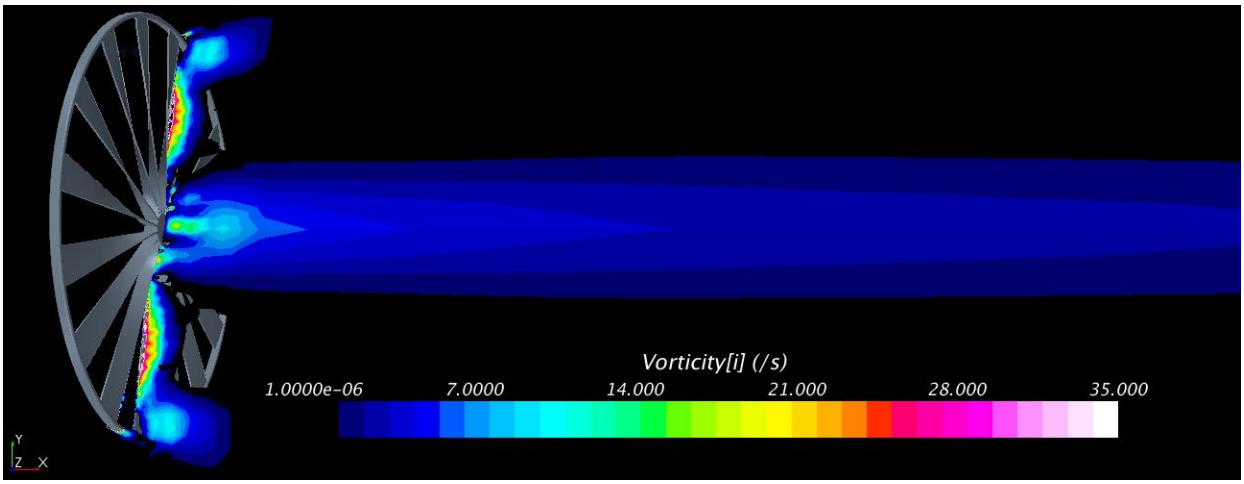

Figure 23: Vorticity contours obtained with the SST model in the 10Dx10Dx10D domain.

VII. Conclusions

In the paper, the results of the flow simulation around and behind the mid-sized Keuka Rim-Driven Wind Turbine developed by Keuka Energy LLC are present. Simulations were conducted with two RANS turbulence models: SST and k-ω 2006[4,5] turbulence models. A sensitivity analysis of the simulation results to the simulation parameters was conducted. It was demonstrated that the structured grid of hexahedral cells predicts more realistic flow structure in the turbine far wake, than the unstructured mesh with polyhedral cells does. The computational domain size in the streamwise is of importance. Computational profiles are over-predicted in shorter domains even in the near wake of the turbine. Different turbulence models predict the similar growth rate of the turbine wake, but some discrepancies in the predicted flow structure are observed within the wake. Experimental facilities are currently under constructions at the Idaho National Laboratory to obtain the observational data for the RDWT wake. Once the data are available, the simulation results will be validated against them.

Acknowledgments

Simulations were conducted using the high-performance facilities of the Center for Advanced Research Computing at the University of New Mexico. A part of work was supported by NASA under award NNX12AJ61A and by the Junior Faculty UNM-LANL Collaborative Research Grant. The authors would like to acknowledge support from CD-Adapco for providing STAR CCM+ to the University of New Mexico for academic purposes.

References

[1]Chen, X., and Ramesh K. Agarwal. "Inclusion of a simple dynamic inflow model in the blade element momentum theory for wind turbine application." *International Journal of Energy and Environment*, Vol. 5.2, 2014, 183-196.

[2]Rankin, A. J., Poroseva, S. V., and Hovsapian, R. O., "Power Curve Data Analysis for Rim Driven Wind Turbine," *ASME Early Career Technical Journal*, 2011, Vol. 10, pp. 27-32.

[3]Sanderse, B., van der Pijl, S. P., and Koren, B., "Review of Computational Fluid Dynamics for Wind Turbine Wake Aerodynamics," Wind Energy, 2011, Vol. 14, pp.799-819.

[4]Menter, F. R., "Zonal Two Equation k-omega Turbulence Models for Aerodynamic Flows," AIAA Paper 93-2906, 1993.

[5]Wilcox, D.C., *Turbulence Modeling for CFD*, 3rd Edition, 2010.

[6]Kaiser, B. E., Poroseva, S. V., Snider, M. A., Hovsapian, R. O., Johnson, E., " Flow Simulation Around a Rim-Driven Wind Turbine And In Its Wake," the 58th ASME Turbo Exposition Proceed., San Antonio, TX, June 3-7, 2013.

[7]Kaiser, B. E., Poroseva, S. V., Johnson, E., Hovsapian, R. O., "Near-Wake Flow Simulations for a Mid-Sized Rim Driven Wind Turbine," AIAA-2013-2419, *Proc. the 43th AIAA Fluid Dynamics Conference*, San Diego, CA, June 24-27, 2013.

[8]STAR-CCM+. Ver. 6.02.007, CD-Adapco, http://www.cd-adapco.com/

[9]Snider, M. A., and Poroseva, S. V., "Sensitivity Study of Turbulent Flow Simulations Over a Rotating Disk," AIAA-2012-3146, *Proc. the 42nd AIAA Fluid Dynamics Conference and Exhibit*, New Orleans, June 25-28, 2012.

[10]Burton, Tony. *Wind Energy: Handbook*. Chichester: J. Wiley, 2001. Chap 1.